

Cooling of high power density electrical drive units for mobile machinery

Christoph Ellenrieder¹, Benedikt Reick¹ and Marcus Geimer²

¹ Hochschule Ravensburg-Weingarten, Weingarten, Deutschland

E-Mail: christoph.ellenrieder@rwu.de; Tel.: (+49)751 501 9656

² Institutsteil Mobile Arbeitsmaschinen, Karlsruher Institut für Technologie, Karlsruhe, Deutschland

Abstract

In this proceeding the demand for a high power density of drives in mobile machinery and their constraints are described. To achieve a high power density with electrical machines liquid cooling is a favoured option. Usually it is state of the art to use cooling jackets in those machines due to manufactureability and robustness. The behaviour of often used rectangular channel structures is well known and can be described with basic thermodynamics. Possible improvements by using vortex generators inside the channel of a cooling jacket structure are discussed. A basic dimple geometry is shown and also evaluated for a cooling spiral.

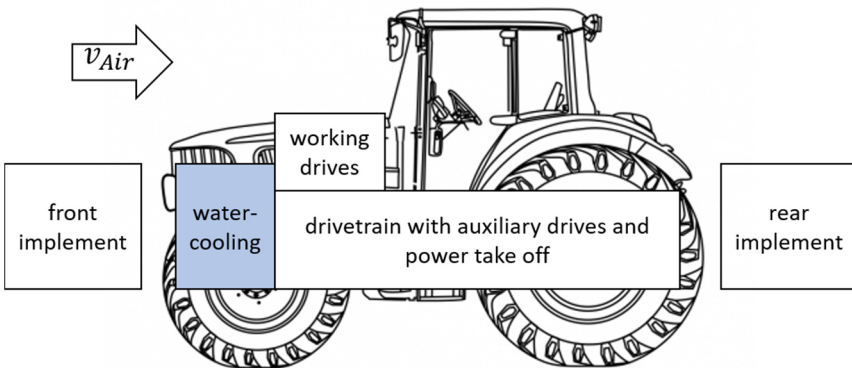
Keywords: power density, cooling of electrical machines, cooling jackets, vortex generator, dimple structures

1 Introduction

The application of electrical machines (EMs) for mobile machinery was analysed in many concepts and tested in prototypes in the past years [1–9]. EMs were used

- as drive unit or wheel hub drives for battery electric machinery,
- as variator drives in electric continuously variable transmissions,
- as drives for mechanical power take offs
- as drives for implements (wheel or working drive)
- and as a generator to supply electrical power for consumers.

Most of the studies conclude with high system efficiencies through the application of EMs. But also, limits of EMs regarding power density and permanent power are stated. Figure 1.1 shows a schematic side view of a tractor with possible positions for EMs. Also boundary conditions for cooling are indicated. For vehicle mounted drives, water and air cooling can be taken into account and for implements, mainly air cooling is suitable.



Tractor picture: happycolorz.de/fahrzeuge/tractor, 11/2020

Figure 1.1: Schematic side view of a tractor.

An analysis of the used drives results in Table 1.1, which compares two positions of EMs, on the machine and on the implement. Air-cooling for EMs on mobile machinery is limited by poor air flow due to low relative speeds or if the EM is cooled by a fan, contamination (e.g. dust or mud) is likely to occur. Therefore, a fluid cooling concept for EMs seems attractive, which is substantiated by high power densities and a lack of available space on the tractor. Water and oil could be supplied on a conventional tractor (engine radiator, drivetrain lubrication and cooling). Water supply is basically not available on implements. Hydraulic cooling might be supported on the implement [10].

Table 1.1: A qualitative comparison of positions and boundary conditions for electric machines on mobile machinery

Boundary condition	EM on tractor	EM on implement
Air flow	o / -	o
Water supply (cooling)	++	--
Oil supply (cooling)	++	+
Contamination	o	--
Electricity supply	+	+
Available space	-	+

Due to this first analysis, the paper focusses on fluid cooled EMs, positioned on the machine itself. Because heat transfer coefficients are normally higher for water than for oil, a water cooling is favoured. Another reason being the high permanent power demand resulting from the fact that a significant amount of energy is required for driving but also in working processes.

The continuous power of EMs, can be described by the S1 duty cycle, which is mainly capsized by heat dissipation described in depth in chapter 2. In chapter 3.1 a short look on thermodynamics gives some insights about parameters which allow to influence the efficiency of the cooling. Furthermore in chapter

3.2 and 3.3 CFD models are prepared and a possibility to optimize a state of the art cooling structure is proposed.

2 Cooling of electrical machines

A comparison between hydraulical and electrical energy conversion involves multiple dependencies for both domains. According to [11–14] the boundary conditions like load profile, cooling situation, available build volume and the mechanical transmission have to be taken into account for EMs.

2.1 Design parameters of electrical machines

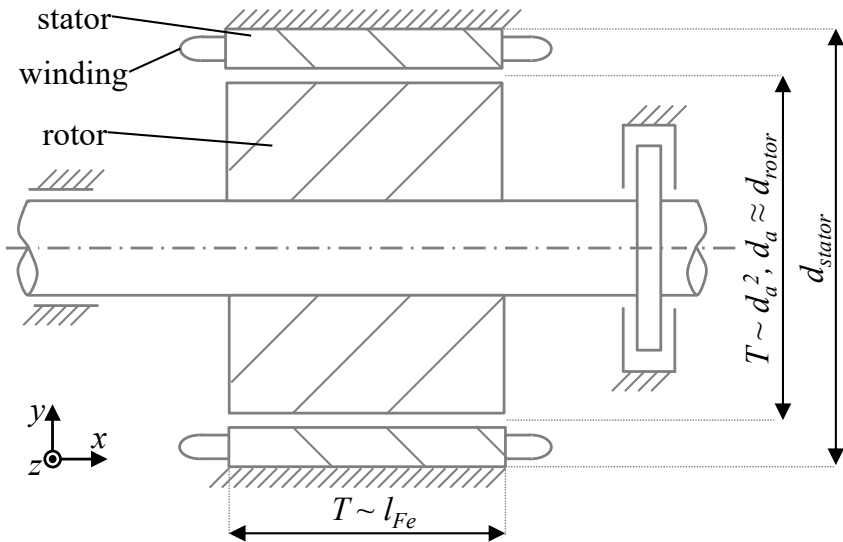


Figure 2.1: Main design dimensions for electrical machines according to [1].

Looking at EMs, depicted in Figure 2.1, the main design parameters are the air gap diameter d_a and active length l_{Fe} of the iron core. Furthermore the outer diameter including the stator and the total length including the winding heads are depending on d_a and the pole number p .

To estimate the torque

$$T = \frac{\pi}{2} \cdot \sigma \cdot d_a^2 \cdot l_{Fe} = \frac{1}{2\pi} \cdot C \cdot d_a^2 \cdot l_{Fe} \quad (2.1)$$

available from given dimensions the rotary thrust σ in $\left[\frac{kN}{m^2}\right]$ or the utilization number C in $\left[\frac{kW \cdot min^{-1}}{m^3}\right]$ have to be taken into account. These quantities have a huge variation where σ is inbetween $25 \text{ kN}/m^2$ to $75 \text{ kN}/m^2$ for a power demand between 10 kW to 1 MW according to [14]. When looking at the influences on the rotary thrust

$$\sigma = \frac{z_c I_c}{\pi \cdot d_a} \cdot B = A \cdot B \quad (2.2)$$

the main parameters that can be influenced in this equation are either the magnetic flux B which is a material parameter due to excitation or the current density A , formed by the number of conductors z_c and the current of one conductor I_c , which is thermally limited and thus is permanent power defining. With a conservative approach from [11] σ is approximately $16.4 \text{ kN}/m^2$ for asynchronous motors (ASM) and $32.2 \text{ kN}/m^2$ for permanent magnet motors (PSM). When looking at the dimensions (d_a, l_{Fe}) of electrical machines and their power output

$$P = 2\pi \cdot T \cdot n = C \cdot d_a^2 \cdot l_{Fe} \cdot n \quad (2.3)$$

the rotational speed n is relevant as well. In different approaches, e.g. [11, 15, 16], n is increased to decrease the build volume as can be seen in Figure 2.2.

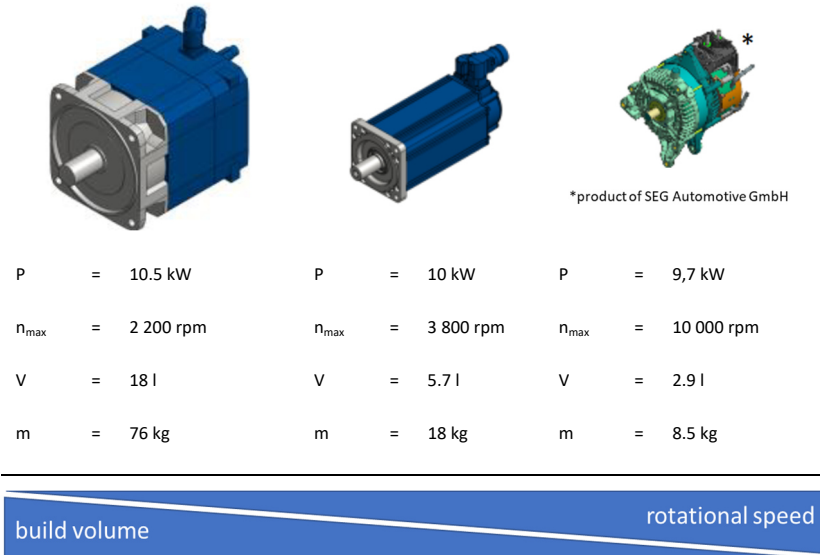


Figure 2.2: Speed dependency of build volume of electrical motors [17–19].

When focusing on the power density only, for these drives a high speed concept seem attractive. Then, in addition high ratio transmissions are required.

Figure 2.3 shows the resulting size comparison of energy converters with similar working conditions (rotational speed, power output, torque) [13]. The electrical drive unit achieves a power density of 916 kW/m³ whereas the hydraulical unit has a power density of 3566 kW/m³.

A blur in this investigation, which is also stated by the author, is that the whole powertrain including e.g. shafts, gears or control-units should taken into account. Also, power density is a function of the volume and not a constant.

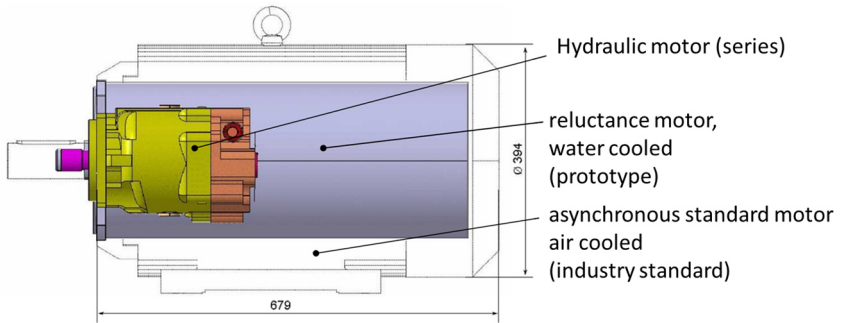


Figure 2.3: Build volume of a hydraulic serial motor, an air cooled and a water cooled electrical machine [13].

2.2 State of the art cooling of electrical machines

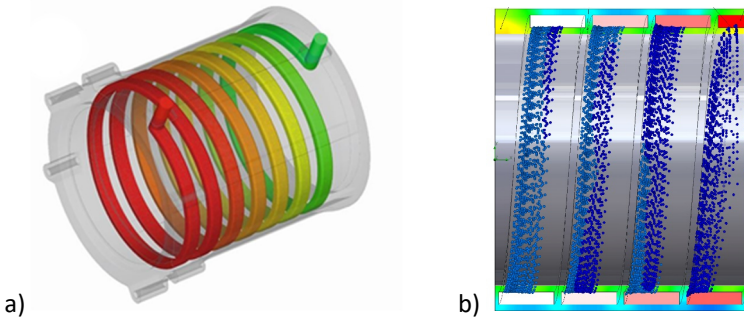


Figure 2.4: a) Axial thermal gradient of a cooling jacket [20] and b) calculated thermal gradient of a cooling jacket.

Currently an often used design for water cooling is the use of a cooling jacket with a water spiral. The advantage of this is a high contact area for cooling and the usage of well-known manufacturing processes e.g. turning and milling. Disadvantageous is that the coolant is moving in only one direction. This results in an axial temperature gradient as can be seen in Figure 2.4. Followed by a

power derating when regarding the maximum temperature of the insulating materials subdividing the conductors is reached at any point, which is classified e.g. with 155 °C for class F or 180 °C for class H.

There are other approaches where the cooling is highly integrated in either the electric conductors [21] or integrated within the winding [22]. Likely disadvantages of those systems are complex manufacturing processes resulting in high cost and mechanical complexity.

Alternatives to the spiral structures in the cooling jacket are being researched in [23], as can be seen Figure 2.5 a), and also manufactured by chill casting in a quite similar approach by Volkswagen in the electric drive unit of the e-Golf [24] shown in Figure 2.5 b). The different shape of the inserted drop-like structure can result from limits like a minimum wall thickness in the casting process.

The casting process of a similar cooling structure is presented as a cheap manufacturing method in [20] where the cooling jacket with the inserted structure is chill casted. The cooling jacket is thermally joined with an also chill casted motor housing.

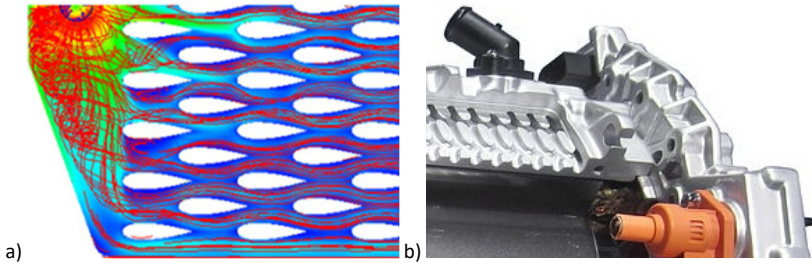


Figure 2.5: a) Alternative cooling structures acc. to [23] and b) sectional model of VW e-Golf electric motor at IAA 2015 [24].

3 Simulation of cooling mechanism

The previously presented approaches are based on complex structures which are examined either by CFD simulations or by testing and measuring the performance of the structure. To get a first impression about the main factors on the cooling, the cooling spiral is broken down into the basics of thermodynamics in the following steps.

3.1 Simplification of a cooling geometry

Assuming the radius of a cooling jacket becomes infinite, the geometry can be interpreted as two plates forming a channel. The effect of curvature will be examined in chapter 3.2.

To calculate the behaviour of a cooling channel mainly consisting of two plates the Reynolds number [25]

$$Re = \frac{w \cdot d_H}{\nu} \quad (3.1)$$

with flow velocity w and viscosity ν is considered. The hydraulic diameter d_H of two plates with distance s can be described as

$$d_H = 4 \cdot \text{circumference} \cdot \text{diameter} = 2 \cdot s. \quad (3.2)$$

The Nusselt number, comparing convective heat transfer to conduction, is

$$Nu = \frac{\alpha \cdot d_H}{\lambda}. \quad (3.3)$$

With constant material properties, the heat transfer coefficient α influences dominantly the heat flux. The heat transfer coefficient α is influenced by geometry, flow type (laminar/turbulent), flow velocity, temperature difference and fluid properties [26]. Corresponding Nusselt numbers are found in literature e.g. [27].

In this case with constant average fluid velocity and constant inlet temperature a temperature profile as shown in Figure 3.1 builds up along the surface. This is the so called thermal boundary layer whose thickness

$$\delta_T \approx \frac{\lambda}{\alpha} = \sqrt{\pi} \sqrt{\frac{a \cdot x}{w_m}} \tag{3.4}$$

increases with the square root of x along the plates and eventually touches other limiting boundary elements.

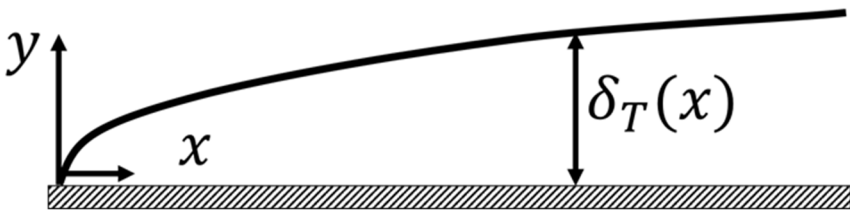


Figure 3.1: Thermal boundary layer of a flow along a plate according to [28].

3.2 Investigation of vortex generators influence on the basic geometry

Carrying out thermal simulations of the above geometry, shows the thermal layering of the coolant in Figure 3.2. As expected, the warm layer is at the bottom and becomes more distinct along the cooling channel.

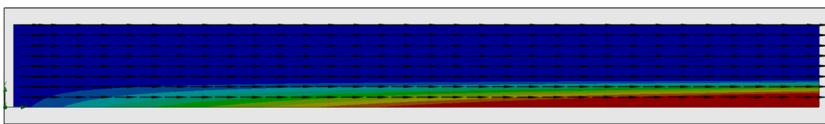


Figure 3.2: Thermal layering of the coolant along the cooling channel.

The convective heat transfer

$$\dot{Q} = A \cdot \alpha \cdot (\vartheta_{Surface} - \vartheta_{coolant}) \quad (3.5)$$

depends on surface area A , heat transfer coefficient α and temperature difference. An increase of heat transfer due to mixing the fluid by vortex generators like dimples can be achieved [29].

In Figure 3.3 the effect of varying dimple depths on the surface temperature are shown by CFD results. In this case, the structure helps to reduce the maximum surface temperature by about 20 K (comparison left to right).

Boundary conditions:

Coolant: $Q = 6 \frac{l}{min}$ @ 20 °C, uniform flow at inlet, $p_{outlet} = 101.3 \text{ kPa}$

Walls: $\dot{Q}_{bottom} = 600 \text{ W}$, others adiabatic, $A_{cooling,surf} = 10000 \text{ mm}^2$

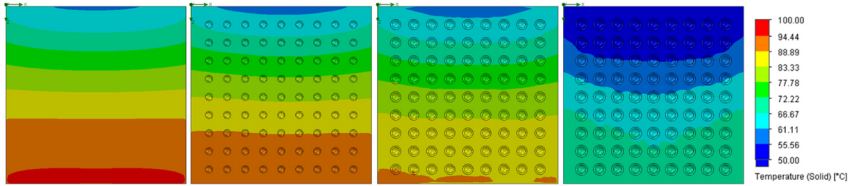


Figure 3.3: Reduction of the surface temperature by the use of dimples with varying depth (left: no dimples, right: dimples with maximum depth).

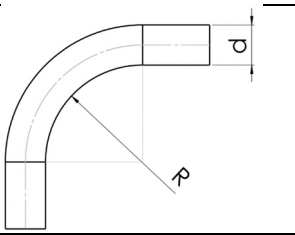
3.3 Influence of a vortex generator in a cooling spiral

The previous approach does not take into account the forces (e.g. centrifugal forces) due to the curvature of the channel which results in a higher pressure drop, showing in the pressure loss coefficient ζ in Table 3.2 but also an increased mixing of the coolant. The pressure loss of this part is proportional [30] with density ρ and velocity v by

$$\Delta p \sim \zeta \cdot \rho \cdot v^2. \quad (3.6)$$

Table 3.2: ζ -values for curvatures of pipes with 90° bend [31]

R/d		1	2	3	4
ζ -value	even	0.21	0.14	0.11	0.09
	rough	0.51	0.30	0.23	0.18



The literature mainly describes pipes in this context. To investigate the behaviour of the coolant in a squared channel spun as a spiral, a CFD simulation using the model shown in Figure 3.4 a) was conducted. The flow of the coolant is indicated in Figure 3.4 b) by the red arrow. The results are shown for one winding of a spiral from the sideview. In Figure 3.5 the spiral without dimples is shown. It represents a state of the art cooling jacket. In this case the coolant temperature is increased from 20 °C at the inlet to approx. 25 °C whereas the inner wall has a peak temperature of approx. 90 °C. When adding dimples to the structure, the outlet temperature of the coolant slightly increases but the inner wall temperature sees a drop in the maximum temperature of about 7 °C, see Figure 3.6. Pressure drops should be paid attention to when adding vortex generators. In this case the slightly increased pressure drop can be neglected.

Boundary conditions:

Coolant: $Q = 6 \frac{l}{min}$ @20 °C, uniform flow at inlet, : $p_{outlet} = 101.3 \text{ kPa}$

Walls: $\dot{Q}_{innerSpiral} = 2500 \text{ W}$, others adiabatic, $A_{cooling,surf} = 66628 \text{ mm}^2$

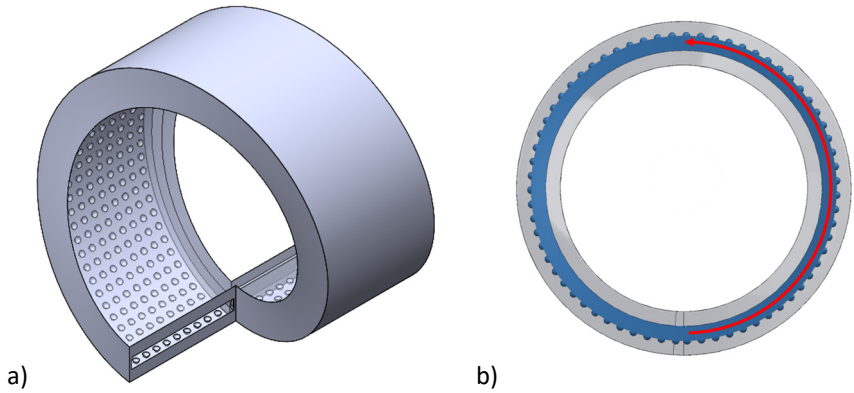


Figure 3.4: a) isometric view of a single cooling spiral turn with dimples and b) side view of spiral turn with flow direction.

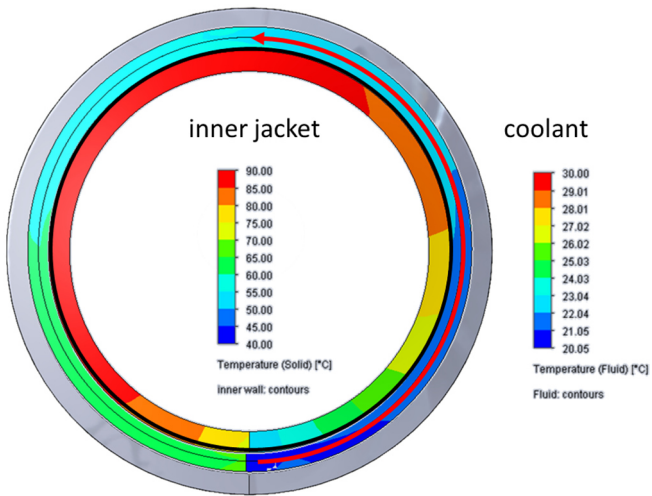


Figure 3.5: coolant and surface temperatures for a spiral cooling jacket.

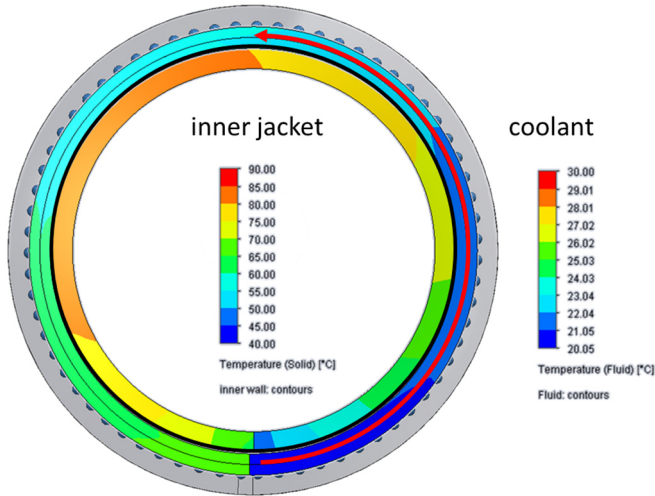


Figure 3.6: coolant and surface temperatures for a spiral cooling jacket with added vortex generators.

4 Conclusion and outlook

In this proceeding an overview about the basic design parameters for EMs was given. It was shown that the cooling is an important part of EMs and the state of the art in research and industry was presented. In the next steps the basic approach to calculate the cooling in channels was described. The mechanics of dimples to improve the performance of the cooling was looked into. For a square channel an advantage of a 20 K cooler surface temperature was achieved. When looking at a spiral, with the better mixed coolant compared to the square channel, the implementation of the same dimples still bring an advantage of 8 K.

These investigations show that by adding vortex generators to state of the art cooling the performance can be increased. In future studies different vortex

generators will be investigated as well as their distribution. The performance and manufacturability will be evaluated, like for instance the 3D profiles in Figure 4.1.

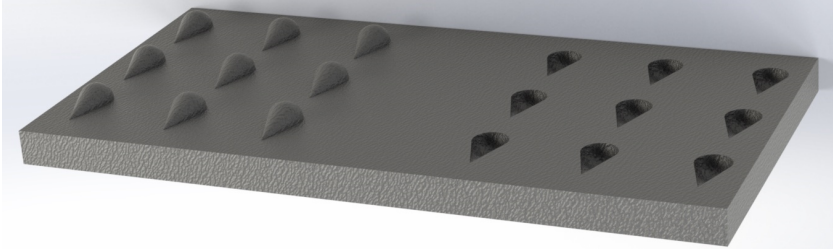


Figure 4.1: Proposed 3D-structures for increasement of turbulences.

Another possibility is to locally add vortex generators to increase Nu near hot spots i.e. like the winding heads. This can help to better utilize the insulating materials by reducing the thermal stress in these hot spots. From this a method to design locally modified heat dissipation can be developed, to adapt the heat transfer coefficient along the cooling channel in such a way that temperature gradients can be reduced or even eliminated.

For such a method distributed loss models of electric motors have to be simulated. These models then have to be evaluated with load profiles and then integrated within CFD simulations resulting in a multi physics simulation.

Modern manufacturing processes like metal 3D printing can be used to create prototypes for these investigations. Finally measurements can be carried out with prototypes to refine simulation models and to verify the simulation results.

The 3D printing technology enables a large spectrum of possible vortex generating structures as there is less limits e.g. for the structures wall thickness in comparison to casting processes. Also the technology allows to vary materials with different heat transfer properties.

References

- [1] B. Reick, Methode zur Analyse und Bewertung von stufenlosen Traktor-getrieben mit mehreren Schnittstellen. Dissertation. Karlsruhe: KIT Scien-tific Publishing, 2018.
- [2] F. Reinmuth, Ermittlung der Potentiale zur Elektrifizierung von Landma-schinen. Dissertation. Aachen: Shaker, 2013.
- [3] M. Wünsche, Elektrischer Einzelradantrieb für Traktoren. Zugl.: Dresden, Techn. Univ., Diss., 2005. Dresden: TUDpress Verl. der Wiss, 2005. [Online]. Available: http://deposit.dnb.de/cgi-bin/dokserv?id=2671900&prov=M&dok_var=1&dok_ext=htm
- [4] R. Gugel, Stufenloser elektromechanisch leistungsverzweigter Antrieb für Arbeitsgeräte, 2009. [Online]. Available: <https://books.google.de/books?id=nh8VSQAACAAJK>. Hahn, Einsatzmöglichkeiten elektrischer Antriebe für landwirtschaftliche Maschinenkombinationen. Zugl.: Hohenheim, Univ., Diss., 2011. Aachen: Shaker, 2011.
- [5] T. Barucki, Optimierung des Kraftstoffverbrauches und der Dynamik eines dieselelektrischen Fahretriebes für Traktoren. Dissertation. Dres-den, 2001.
- [6] M. Götz, M. Fellmann, and K. Grad, "Elektrifizierung und Hybridisierung bei Landmaschinen - Konzepte und Vorteile," in Hybridantriebe für mo-bile Arbeitsmaschinen: 4. Fachtagung [des VDMA und des Karlsruher In-stituts für Technologie], 20. Februar 2013, Karlsruhe, 2013.
- [7] B. Pichlmaier, W. Breu, and A. Szajek, "Elektrifizierung bei Traktoren," (in De;de), ATZ Offhighway, vol. 7, no. 1, pp. 78–88, 2014, doi: 10.1365/s35746-014-0155-x.

- [8] M. Heckmann, Vergleichende Untersuchungen an hydraulischen und elektrischen Achsantrieben für mobile Arbeitsmaschinen unter Berücksichtigung betriebstypischer Einsatzbedingungen. München, 2015.
- [9] M. Geimer and C. Pohlandt, Grundlagen mobiler Arbeitsmaschinen: KIT Scientific Publishing, 2014. Accessed: Oct. 30 2019.
- [10] Svetlana Zhitkova, Björn Riemer, David Franck, Kay Hameyer, and Richard Zahoransky, "Hochdrehzahlmotoren für mobile Arbeitsmaschinen," in Hybridantriebe für mobile Arbeitsmaschinen: 4. Fachtagung [des VDMA und des Karlsruher Instituts für Technologie], 20. Februar 2013, Karlsruhe, 2013, pp. 113–123. Accessed: Nov. 7 2019. [Online]. Available: <https://publikationen.bibliothek.kit.edu/1000033474>
- [11] R. Fischer, Elektrische Maschinen, 13th ed. München: Hanser, 2006.
- [12] M. Gallmeier, Vergleichende Untersuchungen an hydraulischen und elektrischen Baugruppenantrieben für landwirtschaftliche Arbeitsmaschinen. München, 2000.
- [13] E. Hering, R. Martin, J. Gutekunst, and J. Kempkes, Eds., Elektrotechnik und Elektronik für Maschinenbauer. Berlin, Heidelberg: Springer Berlin Heidelberg, 2012.
- [14] T. Pietrzyk, K. Schmitz, S.-R. Lee, D. Roth, and G. Jacobs, "Entwicklung und Auslegung einer elektro-hydraulischen Achse mit einem 48 V High-Speed-Antrieb zur Dezentralisierung der Arbeitshydraulik eines Kompaktbaggers," in Karlsruher Schriftenreihe Fahrzeugsystemtechnik, vol. 67, Hybride und energieeffiziente Antriebe für mobile Arbeitsmaschinen : 7. Fachtagung, 20. Februar 2019, Karlsruhe, W. V. f. M. Wissenschaftlicher Verein für Mobile Arb, Ed., Karlsruhe, Baden: KIT Scientific Publishing, 2019.

- [15] D. J. Roth, G. Jacobs, A. Kramer, M. Krech, T. Pietrzyk, and K. Schmitz, "Bauraumreduktion durch Drehzahlenhebung – Einsatz von High-Speed-Antrieben in elektro-hydraulischen Linearaktuatoren für mobile Anwendungen," in *Karlsruher Schriftenreihe Fahrzeugsystemtechnik*, vol. 67, *Hybride und energieeffiziente Antriebe für mobile Arbeitsmaschinen : 7. Fachtagung*, 20. Februar 2019, Karlsruhe, W. V. f. M. Wissenschaftlicher Verein für Mobile Arb, Ed., Karlsruhe, Baden: KIT Scientific Publishing, 2019.
- [16] Robert Bosch GmbH, Starter Motors and Generators. [Online]. Available: https://www.bosch-press.de/pressportal/de/media/migrated_download/de/BRS_Broschüre_RZ_de.pdf
- [17] Siemens AG, "1FT7132-5AB74-1NK0: Technisches Datenblatt," *Technisches Datenblatt*, 2018.
- [18] Robert Bosch GmbH, "IndaDyn S MSK071D-0300," *Technisches Datenblatt*, 2018.
- [19] F. J. Feikus, P. Bernsteiner, R. F. Gutiérrez, and M. Łuszczak, "Weiterentwicklungen bei Gehäusen von Elektromotoren," *MTZ Motortech Z*, vol. 81, no. 3, pp. 42–47, 2020, doi: 10.1007/s35146-019-0180-5.
- [20] dynamic E flow GmbH, dynamic E flow — Capcooltech.Capcooltech. [Online]. Available: <https://www.dynamiceflow.com/capcooltech> (accessed: Apr. 3 2020).
- [21] Fraunhofer, Direktgekühlter Elektromotor aus Kunststoff. [Online]. Available: <https://www.fraunhofer.de/de/presse/presseinformationen/2019/februar/direktgekuehlter-elektromotor-aus-kunststoff.html> (accessed: Apr. 3 2020).

- [22] N. Karras, "Optimierung der Wärmeabfuhr eines Fahrzeug-Elektromotors und Auswirkungen auf den Gesamtkühlkreislauf," Dissertation, Institut für Verbrennungsmotoren und Kraftfahrtwesen (IVK), Universität Stuttgart, Stuttgart, 2017.
- [23] Hanno Jelden, Peter Lück, Georg Kruse, Jonas Tausen, "Der elektrische Antriebsbaukasten von Volkswagen," MTZ - Motortechnische Zeitschrift, vol. 2014, no. 2, pp. 14–20, 2014.
- [24] P. Stephan, S. Kabelac, and M. Kind, VDI-Wärmeatlas: Fachlicher Träger VDI-Gesellschaft Verfahrenstechnik und Chemieingenieurwesen, 12th ed., 2019.
- [25] R. Marek and K. Nitsche, Praxis der Wärmeübertragung: Grundlagen - Anwendungen - Übungsaufgaben, 3rd ed. München: Hanser, 2012. [Online]. Available: <http://www.hanser-elibrary.com/action/showBook?doi=10.3139/9783446433205>
- [26] Verein Deutscher Ingenieure; VDI-Gesellschaft Verfahrenstechnik und Chemieingenieurwesen, VDI-Wärmeatlas: Mit 320 Tabellen, 11th ed. Berlin: Springer Vieweg, 2013.
- [27] H. D. Baehr and K. Stephan, Wärme- und Stoffübertragung, 8th ed. Berlin, Heidelberg: Springer Berlin Heidelberg, 2013. [Online]. Available: <http://gbv.eblib.com/patron/FullRecord.aspx?p=1538474>
- [28] J. Chen, H. Müller-Steinhagen, and G. G. Duffy, "Heat transfer enhancement in dimpled tubes," Applied Thermal Engineering, vol. 21, no. 5, pp. 535–547, 2001, doi: 10.1016/S1359-4311(00)00067-3.
- [29] H. Dubbel, J. Feldhusen, and K.-H. Grote, Eds., Dubbel: Taschenbuch für den Maschinenbau, 24th ed. Berlin: Springer, 2014. [Online]. Available: <http://search.ebscohost.com/login.aspx?direct=true&scope=site&db=nlebk&db=nlabk&AN=859646>

- [30] L. Böswirth, Technische Strömungslehre: Lehr- und Übungsbuch, 7th ed. Wiesbaden: Friedr. Vieweg & Sohn Verlag / GWV Fachverlage GmbH Wiesbaden, 2007.